Open Access Library Journal
2025, Volume 12, e13866
ISSN Online: 2333-9721
ISSN Print: 2333-9705

A Full Width at Half Maximum (FWHM) Based Approach to Treatment Planning System Validation for Precise Stereotactic Radiotherapy

Nicolas J. Rovetto[1], Lethukuthula N. Ntombela[1,2], Lerato Mohlafase[2], Gezani Isaac Shivambu[1,2]

[1]Department of Medical Physics, Steve Biko Academic Hospital, Pretoria, South Africa
[2]Department of Medical Physics, University of Pretoria, Pretoria, South Africa
Email: nickyrov@gmail.com

How to cite this paper: Rovetto, N.J., Ntombela, L.N., Mohlafase, L. and Shivambu, G.I. (2025) A Full Width at Half Maximum (FWHM) Based Approach to Treatment Planning System Validation for Precise Stereotactic Radiotherapy. *Open Access Library Journal*, **12**: e13866.
https://doi.org/10.4236/oalib.1113866

Received: June 27, 2025
Accepted: August 3, 2025
Published: August 6, 2025

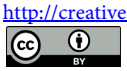

Abstract

Accurate characterization of small radiation fields is essential for high-precision radiotherapy techniques such as Stereotactic Radiosurgery (SRS). This study evaluates the effectiveness of Full Width at Half Maximum (FWHM) analysis as a method for validating a Treatment Planning System (TPS), particularly for detector-dependent variations in small-field dosimetry. Beam profiles and percent depth dose (PDD) data were collected for field sizes ranging from 1×1 cm^2 to 4×4 cm^2 using three detectors, PTW Semiflex 3D, PinPoint 3D, and microdiamond, and compared to Monte Carlo-generated data from the Monaco TPS. An analysis was done of the FWHM results obtained from each detector and from the TPS. The decrement line method was implemented to analyse isodose widths derived from these measurements, as an extra means of comparison. Results show that discrepancies between measured and TPS-predicted FWHM values increase with decreasing field size, with the microDiamond detector showing the largest deviations. However, when full beam dosimetry (including PDD data) was considered, the isodose distributions exhibited closer agreement across the detectors. These findings emphasize the importance of detector selection during commissioning, as well as the role of FWHM and isodose analysis in enhancing TPS validation, QA processes, and ultimately clinical safety in small-field radiotherapy.

Subject Areas

Oncology

Keywords

Full Width at Half Maximum (FWHM), Small-Field Dosimetry, Treatment Planning System (TPS) Validation, Monte Carlo, Radiation Detectors, Decrement Line Method

1. Introduction

The primary objective in radiotherapy is to deliver a high radiation dose to the tumor while minimizing exposure to the surrounding healthy tissues [1]. Achieving this balance requires a comprehensive understanding of the radiation beam's characteristics, which are determined through beam data measurements. However, the accuracy of this data is heavily influenced by the type of radiation detector used during measurement, as it forms the foundation for treatment planning in Treatment Planning Systems (TPS). This becomes especially critical in small-field radiotherapy, where advanced modalities such as Intensity-Modulated Radiotherapy (IMRT), Volumetric Modulated Arc Therapy (VMAT), Stereotactic Radiosurgery (SRS), and Stereotactic Body Radiotherapy (SBRT) are commonly employed [2]. These techniques aim to deliver highly conformal doses to small, well-defined targets with steep dose gradients, necessitating high precision and minimal margins for error.

One of the fundamental parameters in small-field dosimetry is the Full Width at Half Maximum (FWHM), which serves as a key metric in beam profile characterization [3] [4]. In treatments like SRS characterized by high doses per fraction, small target volumes, and few treatment sessions, the accurate assessment of beam width is vital to ensuring adequate tumor coverage while sparing adjacent organs at risk (OARs) [5] [6]. Small fields pose unique challenges, including the loss of lateral charged particle equilibrium, detector volume averaging, and source occlusion. These phenomena can lead to significant dosimetric errors if not properly accounted for [5]-[7]. Detector volume, in particular, plays a crucial role in FWHM accuracy; larger detectors, such as conventional ionization chambers, tend to average the dose over a wider area, resulting in artificially broadened beam profiles and blurred penumbra regions [8]. Conversely, small-volume detectors like the microDiamond offer superior spatial resolution and produce FWHM values that closely align with Monte Carlo simulations and geometric expectations [9].

Moreover, the measured FWHM often deviates from the nominal field size in small-field setups due to effects such as source occlusion and penumbra overlap [10] [11]. These deviations can affect the percentage depth dose (PDD) curves and contribute to errors in dose calculation if not properly understood and corrected. FWHM is also integral to the validation of TPS beam modelling. Accurate small-field dose calculations rely on benchmarked beam profiles, and discrepancies between measured and TPS-predicted values can indicate issues with machine cali-

bration, detector appropriateness, or algorithm accuracy. In this study, small-field beam profiles ranging from 1×1 cm^2 to 4×4 cm^2 were measured using three types of detectors: the Semiflex 3D ionization chamber, the PinPoint 3D chamber, and the microDiamond detector. These measurements were compared with Monte Carlo-based profiles generated by the Monaco TPS to evaluate both measurement fidelity and modelling precision. The study's main goal is to quantify FWHM in small-field radiotherapy to improve dose delivery accuracy and protect healthy tissues. The decrement line method was applied to assess how detector choice influences isodose curve characteristics, offering further insight into TPS reliability and detector-induced variations. Additionally, FWHM serves as a critical tool in quality assurance (QA) and linac commissioning, helping verify beam symmetry, alignment, and output stability factors that are especially vital in high-gradient small-field applications.

2. Materials and Methodology

2.1. Data Collection

Both raw data and Monte Carlo-simulated data from the Monaco TPS were collected. These processes are outlined in this section. The materials used to collect the raw data included the three radiation detectors, as listed in Table 1, as well as a PTW Beamscan water phantom, used together with the PTW Trufix positioning tools. An Elekta Versa HD linear accelerator was used to collect the raw data. The TPS data from the Monaco TPS was generated using the same set-up parameters that were used when collecting the raw data. Python was used for analyses. Once the raw data was obtained, each of the data sets was used to analyse the isodose distributions generated by the data sets, by making use of the decrement line method, which was also coded in Python.

2.1.1. Measurements with Detectors

The three radiation detectors that were used to collect the raw data have been included in Table 1.

Table 1. Radiation detectors used to collect raw data [12]-[14].

DETECTOR	TYPE	SENSITIVE VOLUME	SENSITIVE RADIUS
PTW Semiflex 3D [12]	Ionization chamber	0.07 cm^3	2.40 mm
PTW PinPoint 3D [13]	Ionization chamber	0.016 cm^3	1.45 mm
PTW microdiamond [14]	Solid state detector	0.004 mm^3 (0.000004 cm^3)	1.10 mm

For each detector, data was collected using the same Elekta Versa HD linear accelerator and the same set-up parameters. The phantom that was used was the PTW Beamscan water tank and the detectors were positioned using the PTW Trufix detector positioning tools. The "Auto Beam-Adjustment" functionality of the PTW Beamscan tank was used to automatically find the central position of the radiation beam, for each detector, before taking the measurements. The set-up

parameters that were used are included in Table 2.

Table 2. Set-up parameters that were used to collect the raw data.

SET-UP PARAMETERS	
Source to Surface Distance (SSD)	100 cm
Photon Energy	6 MV
Field-Size	1×1 cm^2, 2×2 cm^2, 3×3 cm^2, 4×4 cm^2
Measurement Depth (for beam profiles)	10 cm

The beam profile data were collected for each of the detectors, and for each field size. Percentage-depth-dose (PDD) data was also obtained for each detector and field-size. Continuous scans were taken, using the smallest resolution available for each of the detectors. Each measurement was repeated three times, and an average between the three was obtained. There were no large or noticeable discrepancies between the repeated measurements.

2.1.2. Monaco Treatment Planning System Data

The same experimental set-up that was used to collect the raw data was replicated on the Monaco TPS to obtain the Monte Carlo-generated data. The dose distribution was calculated, and the dose data was extracted, using the method explained below.

A uniform phantom ($30 \times 30 \times 30$ cm^3 cube) was imported into Monaco, contoured, and assigned a uniform electron density equivalent to water. A single anteroposterior (AP) beam was created, prescribing 1.0 Gy to the center of the phantom at a depth of d_{max} (1.5 cm). The source-to-surface distance (SSD) was set to 100 cm using an initial field-size of 4×4 cm^2. The Monte Carlo dose calculation algorithm was used to calculate the dose distribution, using a calculation matrix of 0.1 mm and an error threshold of 0.5%. After the dose was calculated, coronal dose planes were exported at a depth of 10 cm (matching the experimental set-up). Additionally, a transverse dose plane passing through the center of the phantom was exported. The exported dose planes were analysed using the PTW VeriSoft software, which extracted the beam profiles from the coronal dose planes and the PDD data from the transverse dose planes. This process was repeated for all of the other field sizes that were used when collecting the raw data.

2.2. Isodose Lines Generation (Decrement Line Method)

The isodose distributions generated by the different sets of data were investigated as an additional means of comparing the detectors to each other and to the TPS data, as well as to compare the deconvolved data to the TPS data. The "decrement lines" process, originally described in a thesis submitted by Hidaytalla [15], was used for this analysis. The exact process that was implemented, which was coded in Python, is described by Ntombela *et al.* [16] in their paper which evaluated the effects that different detectors have on the penumbra re-

gion of beam profiles.

3. Results

TPS Data Versus Raw Data

The raw results include the measured beam profile data as well as the same data sets obtained from the TPS, generated using Monte Carlo. The raw profiles have been plotted against the TPS profiles, for each field-size, as shown in Figure 1. To obtain the final raw profiles and PDDs, the three repeated measurements of each data set were averaged. The resultant FWHM results and other results that were extracted from these were extracted from the averaged beam-profiles and PDDs. The point-wise standard deviations between the repeated measurements ranged from 0.000041% to 0.0542% across the data sets (including the beam-profiles and PDDs), with a mean standard deviation of 0.0092%.

Python was used to process the measured data. To obtain the FWHM for each beam-profile, the dose data was first interpolated using a linear method to generate a finer resolution of 1000 points across the measured profile range, to improve the accuracy in identifying the half-maximum points. The maximum dose was then identified for the interpolated profile, and the half-maximum value was defined as 50% of this maximum. The algorithm then located the two positions where the profile crossed this half-maximum value (on the left-hand side and right-hand side of the profile). A final linear interpolation was then performed between the surrounding dose points to precisely determine these crossing positions. The FWHM was then finally calculated as the absolute distance between these two half-maximum points, representing the FWHM.

Table 3 shows a comparative analysis of the FWHM measurements between the TPS data and the raw data obtained from each of the three detectors, for each field-size that was measured. The TPS serves as a reference for ideal or benchmark FWHM values, and the deviations between these and those of the raw data from each detector have been calculated. As the field-size decreases, the discrepancy between the TPS data and the detector measurements generally increases, with the microDiamond detector showing the largest percentage deviations, most notably for the smaller field-sizes. The deviations that are experienced highlight the impact of the detector characteristics on the dose profile accuracy, particularly in small-field dosimetry.

Table 3. FWHM results for raw data versus TPS data.

FIELD SIZE (cm^2)	TPS DATA FWHM (mm)	SEMIFLEX 3D		PINPOINT 3D		MICRODIAMOND	
		FWHM (mm)	DEV.	FWHM (mm)	DEV.	FWHM (mm)	DEV.
4 × 4	42.80	42.49	0.72%	42.20	1.40%	42.26	1.26%
3 × 3	32.21	31.87	1.06%	32.05	0.49%	31.56	2.04%
2 × 2	21.84	21.37	2.15%	21.52	1.46%	21.06	3.58%
1 × 1	12.07	11.23	6.91%	10.79	10.60%	10.55	12.59%

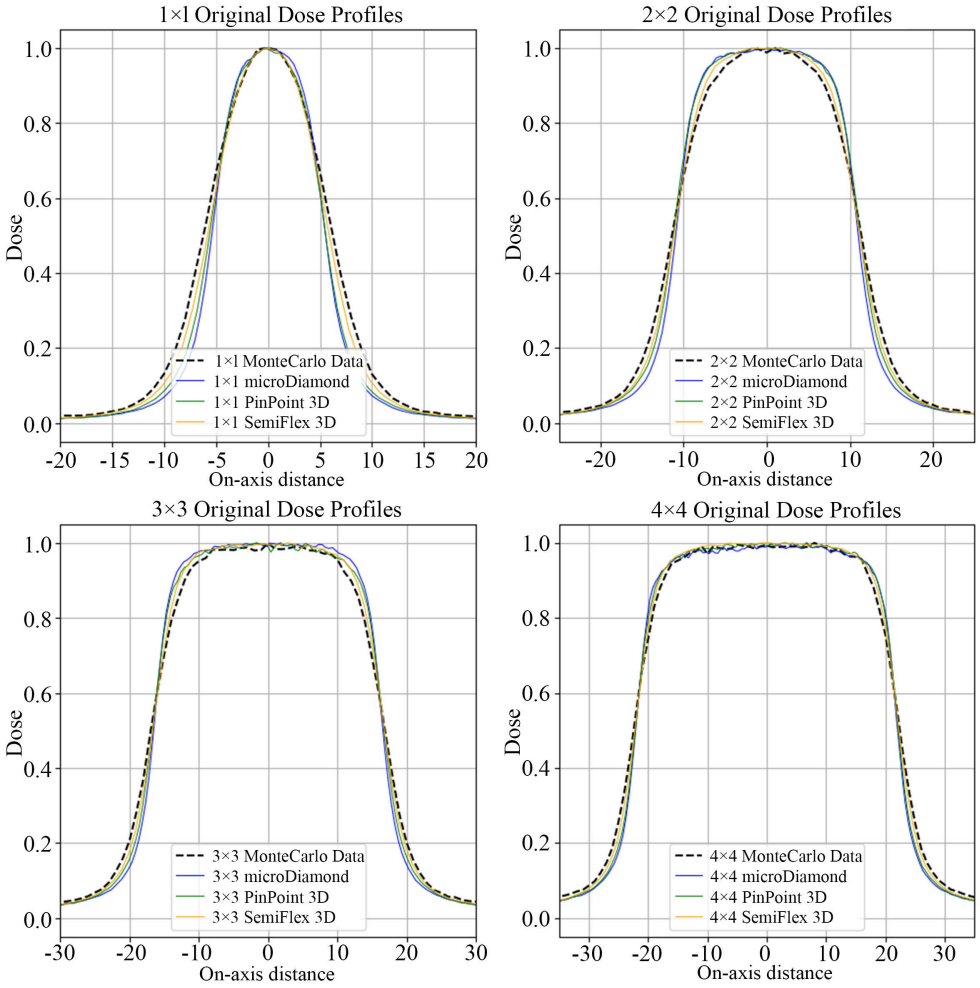

Figure 1. Monte Carlo TPS beam profiles versus raw beam profiles for each detector and field size.

4. Discussion

4.1. FWHM

The comparison of the FWHM values in Table 3 between the Monte Carlo-generated data and the measured raw data for each of the detectors demonstrates noticeable discrepancies. These deviations showcase the impact of detector choice on accurately characterizing the FWHM and the beam-edges, specifically when dealing with small-fields.

For the larger field-sizes (3×3 cm^2 and 4×4 cm^2), all of the detectors showcase a relatively close relation to the Monte Carlo data, with the largest discrepancy being 2.04% for the microDiamond chamber and the 3×3 cm^2 field-size. As the field-size decreases, particularly to the 1×1 cm^2 level, there is a noticeable increase in the discrepancy from the Monte Carlo data across all of the chambers. All of the chambers tend to underestimate the FWHM when compared to the Monte Carlo data. The narrower FWHM for the smaller detectors suggests a higher spatial resolution, but also indicates the potential for underestimation of the true FWHM due to their smaller sensitive volumes.

The Semiflex 3D, which has the largest sensitive volume, showcases the closest similarity for the smaller field-sizes, with deviations of 2.15% and 6.91% for the 2 × 2 cm^2 and 1 × 1 cm^2 field-sizes, respectively. Conversely, the microDiamond detector, with the smallest sensitive volume, showcased the largest deviations for these small fields, with values of 3.58% and 12.59% for the 2 × 2 cm^2 and 1 × 1 cm^2 field-sizes, respectively. This is likely due to the fact that the comparison was made between the profile from the TPS, which is influenced by the commissioning measurements, which were collected using a Semiflex 3D detector. Thus, even though the spatial resolution of the smaller detectors is greater, the benchmark was taken by a detector with a larger volume, leading to larger discrepancies for the smaller-volume detectors.

When performing quality assurance measurements using this type of method, it would be recommended to use the same type of detector that was used during commissioning, if comparing with the TPS Monte Carlo data, which is the Semiflex 3D detector in our case. The results indicate that, for other detectors, you can not fully rely on the TPS generated Monte Carlo data, as it is heavily based on the commissioning measurements. The Monte Carlo dose calculation engine within the Monaco TPS was configured with a statistical uncertainty (variance) of 0.5% per calculation point and a dose grid resolution of 0.1 mm, using a beam with a clinical source model pre-commissioned by Elekta. While this configuration ensures high spatial resolution and low statistical noise in the resulting dose distribution, it remains dependent on the commissioning data – specifically, the beam profiles measured with a Semiflex 3D ionization chamber. Due to this, even though the TPS-generated Monte Carlo data provides a realistic clinical representation, it is not fully independent of the linear accelerator used to perform the measurements. In contrast, it would be recommended to also compare to "true Monte Carlo" simulations, which would be derived purely from fundamental particle transport without reliance on measured input data. This would offer an unbiased benchmark for comparison of the detectors.

Clinically, millimetre-scale FWHM errors at steep dose gradients translate directly to underdosage of the target, or overdosage of adjacent healthy tissues. Doing this sort of analysis of the FWHM using different detectors directly challenges the TPS beam modelling, especially in small-fields. This is done by revealing under- or over-estimation trends. This work also highlights the importance of ensuring accuracy during the commissioning process, and using as many means as possible to validate those measurements. Even small deviations in the commissioning data could propagate into TPS inaccuracies if the raw data is not properly corrected or selected. This is a good method to validate such systems, particularly for advanced treatments like SRS.

4.2. Isodose Lines

The decrement lines process was used to generate the isodose distributions of each of the raw data sets, as well as of the Monte Carlo TPS data. The process takes into

account the beam-profiles, as shown in Figure 1, but also the PDD curves measured for each of the detectors and for the TPS data. This was done for the 50% isodose line, which characterizes the FWHM, as well as a higher isodose that is commonly of interest in treatment planning, the 90% isodose line. The distributions were generated assuming circular symmetry, due to the small field-sizes that we are concerned with. In practise, and especially when dealing with larger field-sizes, including diagonal beam-profile data in this analysis could serve as an extra means for comparison. The isodose lines were generated at a depth of 5 cm, for a 1×1 cm^2 field-size, and have been plotted for each detector, as well as for the TPS data. The deviations experienced for each of the isodose values and each detector are given in Table 4.

Table 4. Isodose line deviations between TPS data and measured data for each detector.

ISODOSE	TPS (mm)	SEMIFLEX 3D		PINPOINT 3D		MICRODIAMOND	
		DIST (mm)	DEV. (mm)	DIST (mm)	DEV. (mm)	DIST (mm)	DEV. (mm)
50%	6.39	5.27	1.12	5.46	0.93	5.25	1.14
90%	0.97	1.87	0.90	1.57	0.60	1.87	0.90

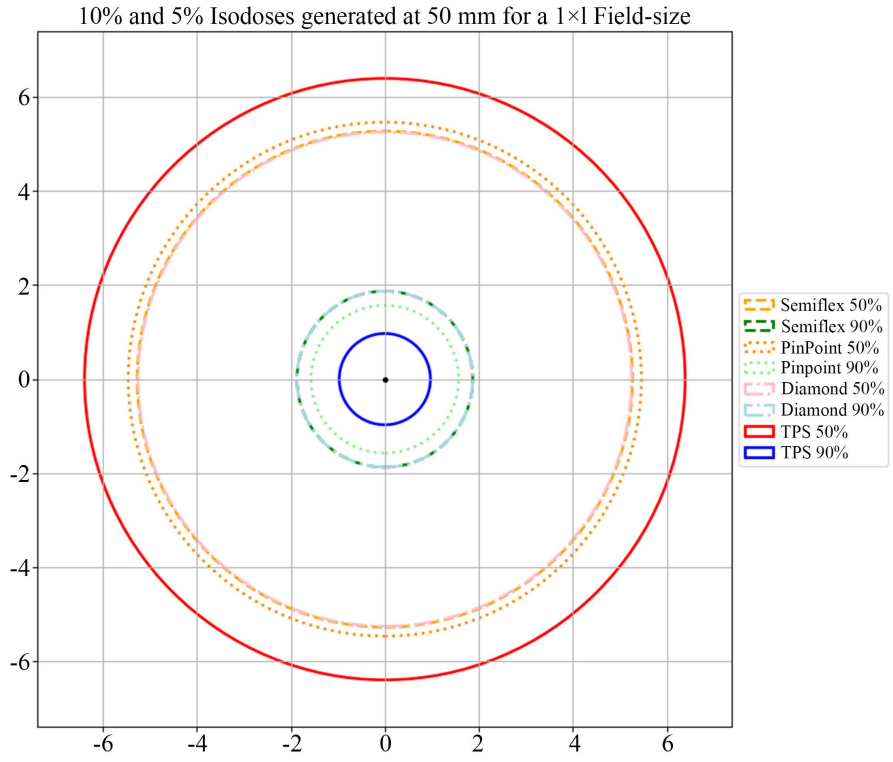

Figure 2. Isodose lines generated using the decrement line method for the TPS data and measured data for each detector.

It can be seen in Figure 2 and Table 4 that, even though the detectors, particularly the microDiamond, demonstrated large deviations when comparing the direct FWHM, the isodoses generated using the decrement lines process were rela-

tively consistent, and are close to 1 mm for each of the detectors when considering the 50% isodose lines. This 1 mm deviation is noticeable, however, especially when dealing with such a small-field. When implementing the full process and considering the PDD curves that were measured with each detector, the final isodoses showcased closer results between each of the detectors than for the direct FWHM comparisons. This indicates that when considering the full dosimetry of the beam, not only the lateral components through the beam profiles, the accuracy tends to increase. The deviations for the 90% isodoses were even closer to the Monte Carlo data, with the largest being 0.9 mm for the Semiflex 3D and microDiamond detectors. This shows the importance of including all aspects of the beam when doing final treatment planning, to ensure accurate dosimetry and tumour coverage.

Incorporating similar decrement-line method analysis as part of routine QA could serve as a beneficial additional means to validate the commissioning data at different frequencies. Collecting the data needed can provide a rapid, intuitive QA check of beam symmetry, penumbra tightness, FWHM accuracy, and alignment integrity. These can then be compared to previous data as a means of validating consistency of the beam.

4.3. Study Limitations

There are various aspects of this study which serve as limitations which may influence the interpretation of the results and their direct applicability to clinical settings. Firstly, all measurements and TPS simulations were conducted using a homogeneous water-equivalent phantom, which does not account for the complexities of tissue inhomogeneities found in actual patients. This might impact the possibility of generalising the FWHM and isodose finding in anatomically diverse treatment sites. Secondly, the decrement line method used to generate the isodose distributions assumed circular symmetry of the radiation field (for small-fields), which may not accurately represent beam characteristics in fields affected by beam-shaping devices or anatomical irregularities. While this assumption is reasonable for small, symmetric fields, it introduces potential inaccuracies for more complex scenarios in a clinical setting. Thirdly, each measurement was only repeated three times, which limits the robustness of the statistical analysis and may not fully capture the extent of measurement variability. However, relatively low variations were experienced during the measurements, which is common (and wanted) when performing beam-profile or PDD measurements on the same linear accelerator.

5. Conclusion

When dealing with stereotactic radiosurgery, where treatment precision is vital and dose gradients are steep, the accurate characterization of beam profiles becomes a clinical necessity rather than a technical formality. This study highlights the pivotal role of FWHM analysis in validating treatment planning systems, particularly when small field-sizes are employed. As introduced, the choice of radiation detector influences the measured beam profile, and consequently the FWHM,

due to variations in spatial resolution and volume-averaging effects. These differences, if not properly accounted for, can propagate through the treatment planning process and affect accurate dose delivery.

By comparing the FWHM values obtained from the three different radiation detectors against the Monte Carlo-based TPS data, it became evident that discrepancies grow more profound with decreasing field-sizes, underlining the importance of selecting appropriate detectors during beam data commissioning. It also became clear that the detector used during commissioning heavily affected the TPS Monte Carlo data that was generated, leading to the Semiflex 3D results being the closest to the TPS. It would be recommended to use true theoretical Monte Carlo data to properly compare with each of the radiation detectors. For QA purposes, however, if the TPS Monte Carlo data is used, then the same detector (Semiflex 3D in this case) should be used for the comparison.

Clinically, even minor deviations in the FWHM can lead to suboptimal tumour coverage or unintended radiation to adjacent organs at risk or healthy tissues, especially when dealing with high-dose, hypofractionated treatments like SRS. Accurate FWHM measurement ensures that the effective field-size used in planning reflects the actual dose distribution delivered to the patient. Additionally, integrating FWHM analysis into QA and commissioning workflows strengthens confidence in TPS modelling, supporting safer treatment delivery and enhancing patient outcomes.

Ultimately, this study reinforces that precision in small-field dosimetry begins at the fundamental level of beam characterization. Rigorously evaluating the FWHM and its dependence on detector type allows medical physicists to better validate and refine TPS performance, bridging the gap between physical measurement and clinical execution in modern radiotherapy.

Conflicts of Interest

The authors declare no conflicts of interest.

References

[1] Malicki, J. (2012) The Importance of Accurate Treatment Planning, Delivery, and Dose Verification. *Reports of Practical Oncology & Radiotherapy*, **17**, 63-65. https://doi.org/10.1016/j.rpor.2012.02.001

[2] Cmrecak, F., Andrasek, I., Mekic, M.S., Ravlic, M. and Beketic-Oreskovic, L. (2019) Modern Radiotherapy Techniques. *Croatian Journal of Oncology*, **47**, 2-3.

[3] Monasor Denia, P., Castellet García, M.d.C., Manjón García, C., Quirós Higueras, J.D., de Marco Blancas, N., Bonaque Alandí, J., *et al.* (2019) Comparison of Detector Performance in Small 6 MV and 6 MV FFF Beams Using a Versa HD Accelerator. *PLOS ONE*, **14**, e0213253. https://doi.org/10.1371/journal.pone.0213253

[4] Dsouza, R.N., Sharan, K., Sukumar, S., Chandraguthi, S.G., Rao, S., Lewis, S., *et al.* (2025) Comparison and Assessment of Different Small Volume Radiation Detectors for Small Field Dosimetry in Stereotactic Radiotherapy. *Asian Pacific Journal of Cancer Prevention*, **26**, 1343-1351. https://doi.org/10.31557/apjcp.2025.26.4.1343

[5] Podgorsak, E.B., Bruce Pike, G., Pla, M., Olivier, A. and Souhami, L. (1990) Radiosurgery with Photon Beams: Physical Aspects and Adequacy of Linear Accelerators. *Radiotherapy and Oncology*, **17**, 349-358. https://doi.org/10.1016/0167-8140(90)90008-k

[6] Wilcox, E.E. and Daskalov, G.M. (2008) Accuracy of Dose Measurements and Calculations within and beyond Heterogeneous Tissues for 6 MV Photon Fields Smaller Than 4 cm Produced by Cyberknife. *Medical Physics*, **35**, 2259-2266. https://doi.org/10.1118/1.2912179

[7] Sharpe, M.B., Jaffray, D.A., Battista, J.J. and Munro, P. (1995) Extrafocal Radiation: A Unified Approach to the Prediction of Beam Penumbra and Output Factors for Megavoltage X-Ray Beams. *Medical Physics*, **22**, 2065-2074. https://doi.org/10.1118/1.597648

[8] Keivan, H., Maskani, R., Shahbazi-Gahrouei, D., Shanei, A., Pandesh, S. and Tarighati Sereshke, E. (2022) Evaluation of Effective Field Size Characteristics for Small Megavoltage Photon Beam Dosimetry. *International Journal of Radiation Research*, **20**, 163-168. https://doi.org/10.52547/ijrr.20.1.25

[9] Bagheri, H., Soleimani, A., Gharehaghaji, N., Mesbahi, A., Manouchehri, F., Shekarchi, B., Dormanesh, B. and Dadgar, H.A. (2017) An Overview on Small-Field Dosimetry in Photon Beam Radiotherapy Developments and Challenges. *Journal of Cancer Research and Therapeutics*, **13**, 175-185.

[10] Ding, G.X. and Das, I.J. (2023) On the Field Size Definition and Field Output Factors in Small Field Dosimetry. *Medical Physics*, **50**, 3833-3841. https://doi.org/10.1002/mp.16262

[11] Palmans, H., Andreo, P., Huq, M.S., Seuntjens, J., Christaki, K.E. and Meghzifene, A. (2018) Dosimetry of Small Static Fields Used in External Photon Beam Radiotherapy: Summary of TRS-483, the IAEA-AAPM International Code of Practice for Reference and Relative Dose Determination. *Medical Physics*, **45**, 1123-1145. https://doi.org/10.1002/mp.13208

[12] PTW. Semiflex 3D Ion Chamber 31021. https://www.ptwdosimetry.com/en/products/semiflex-3d-ion-chamber-31021

[13] PTW. PinPoint 3D Ion Chamber. https://www.ptwdosimetry.com/en/products/pinpoint-3d-ion-chamber

[14] PTW. MicroDiamond. https://www.ptwdosimetry.com/en/products/microdiamond#c781

[15] Hidaytalla, L.A. (1994) Development of Isodose Curves for a 6MV X-Ray Beam. Master's Thesis, University of Khartoum.

[16] Lethukuthula, N.N., Lerato, M., Nicolas, R.J. and Gezani, S.I. (2025) Performance Evaluation of Ionization Chambers and Microdiamond Detectors in Small Field Penumbra Measurements. *International Journal of Medical Physics, Clinical Engineering and Radiation Oncology*, **14**, 89-99. https://doi.org/10.4236/ijmpcero.2025.143007